Direct Visualization of the Microtubule Lattice Seam Both In Vitro and In Vivo

Masahide Kikkawa, Takashi Ishikawa,* Takao Nakata, Takeyuki Wakabayashi,* and Nobutaka Hirokawa

Department of Anatomy and Cell Biology, Faculty of Medicine; and * Department of Physics, School of Science, University of Tokyo, 7-3-1 Hongo, Bunkyo-ku, Tokyo 113, Japan

Abstract. Microtubules are constructed from α- and β-tubulin heterodimers that are arranged into protofilaments. Most commonly there are 13 or 14 protofilaments. A series of structural investigations using both electron microscopy and x-ray diffraction have indicated that there are two potential lattices (A and B) in which the tubulin subunits can be arranged. Electron microscopy has shown that kinesin heads, which bind only to β-tubulin, follow a helical path with a 12-nm pitch in which subunits repeat every 8-nm axially, implying a primarily B-type lattice. However, these helical symmetry parameters are not consistent with a closed lattice and imply that there must be a discontinuity or "seam" along the microtubule. We have used quick-freeze deep-etch electron microscopy to obtain the first direct evidence for the presence of this seam in microtubules formed either in vivo or in vitro. In addition to a conventional single seam, we have also rarely found microtubules in which there is more than one seam. Overall our data indicates that microtubules have a predominantly B lattice, but that A lattice bonds between tubulin subunits are found at the seam. The cytoplasmic microtubules in mouse nerve cells also have predominantly B lattice structure and A lattice bonds at the seam. These observations have important implications for the interaction of microtubules with MAPs and with motor proteins, and for example, suggest that kinesin motors may follow a single protofilament track.

A microtubule is one of the major cytoskeletal elements that plays important roles in various kinds of basic cellular mechanisms such as organelle transport, mitosis, and cell morphogenesis. Over the past two decades, much research attention has been directed at investigating the structure of a microtubule. Amos and Klug (2) studied the lattice structure of flagellar microtubules, and based on optical diffraction patterns from electron micrographs, they concluded that the A subfiber is comprised of a staggered arrangement of tubulin dimers of neighboring protofilaments, whereas in the B subfiber, the tubulin dimers are obliquely lined up at a shallow angle. On the other hand, in vitro-polymerized, pure microtubules were also studied using EM, and the corresponding tubulin dimers were found to be so similar that their alignment could not be distinguished (6); a discrepancy that may arise due to the additional proteins known to exist in flagellar microtubules, which give rise to some of the larger periodicities observed, e.g., an 8-nm pitch. Even so, the A and B lattices have nevertheless been respectively denoted as the proposed structure for the flagellar A and B subfibers. As for the tubulin monomer arrangement, microtubules must be comprised of a three-start symmetric helix with a helical pitch of 12 nm, provided the number of protofilaments is from 11 to 15 (3, 5). Beese et al. (4) carried out a high-resolution (up to 18 Å) X-ray fiber diffraction study on microtubules, yet still the dimer lattice structures could not be well distinguished due to the similarity of α- and β-tubulins.

Song and Mandelkow (23) subsequently showed that a recombinant kinesin head decoration distinguished the α- and β-tubulins, and as a result, its optical diffraction pattern, supports the conventional B-lattice model. The combination of a three-start helix and B-lattice implies a discontinuity exists somewhere in the microtubule wall (17), i.e., the 12-nm helical pitch and 8-nm longitudinal pitch which occurs between dimers on a protofilament are not multiples of each other. To elucidate the structure of a possibly disordered lattice, previous studies using cryo-EM or negative staining had two major drawbacks. (*a*) The image is a combination of both upper and lower sides. These two can never be separated without assuming some ordered structure. (*b*) The images obtained do not have enough contrast to resolve each macromolecule to elucidate the disordered structure. This led to the present study in which we use quick-freeze, deep-etch EM to visualize the surface of kinesin head-decorated microtubules. Our technique enables macromolecules such as the kinesin head to be observed with sufficient resolution to distinguish their arrangement.

Address all correspondence to N. Hirokawa, Department of Anatomy and Cell Biology, Faculty of Medicine, University of Tokyo, 7-3-1 Hongo, Bunkyo-ku, Tokyo 113, Japan. Tel.: (81) 3 3812 2111 (ext. 3326). Fax: (81) 3 5689 4856.

Materials and Methods

Expression and Kinesin Heads

The head domain of mouse kinesin cDNA (3-340 amino acids [a.a.][1]) (12, 14, 21, 24, 27) was inserted at the BamHI-XhoI sites of the PET21b *Escherichia coli* expression vector (Novagen, Madison, WI), which carries an in-frame six-histidine tag at the COOH terminus for purification. Plasmids were transformed into *E. coli* strain BL21(DE3). The cells were grown for 2 h at 37°C, and harvested after 10 h of induction with 0.4 mM isopropyl β-D-thiogalactoside at 18°C. Then, using a French press that had been cooled to 4°C, they were lysed for two cycles in Tris-HCl buffer (20 mM Tris-HCl, pH 7.9, 500 mM NaCl, 5 mM imidazole). The protein was recovered in a soluble fraction as previously described (21). Purification was carried out according to the manufacturer's instructions using a chelating Sepharose FF column (Pharmacia Fine Chemicals, Piscataway, NJ) and the resultant elution was dialyzed against PEM buffer (100 mM Pipes, pH 6.9, 1 mM $MgCl_2$, 1 mM EGTA). Typically, 100 mg of protein at greater than 90% purity was obtained from 4 g of cell pellet (wet weight).

Preparation of Tubulin

Three-cycled, phosphocellulose-purified tubulin was purified from porcine brains as described elsewhere (8, 22).

Chemical Cross-linking and Western Blotting

Chemical cross-linking was performed at 20°C for 15 min in PEM buffer, 5 mM 1-ethyl-3-[3-(dimethylamino)propyl]carbodiimide (zero-length cross-linker), 10 μM taxol (Drug Synthesis & Chemistry Branch, National Cancer Institute, Bethesda, MD), 1.2 mg/ml of tubulin, 1 mM AMP-PNP, and in the presence/absence of 1.2 mg/ml of kinesin head. The reaction was quenched by a 1/100 vol of 2-mercaptoethanol. The cross-linked protein was loaded onto 7.5% SDS-PAGE and transferred to a PVDF membrane. The sheet was immunoblotted with DM1A and DM1B monoclonal antibodies, followed by peroxidase-conjugated second anti-mouse IgG antibody. We used reagents from Sigma Chemical Co. (St. Louis, MO) unless otherwise stated.

Quick-freeze Deep-Etching of Kinesin–Microtubule Complex

Polymerized microtubules (final 2.4 mg/ml) and excess kinesin heads (final 9 mg/ml) were mixed in PEM buffer supplemented with 10 μM taxol, 1 mM AMP-PNP at 20°C for 10 min, and then ultracentrifuged at 110,000 *g* (50,000 rpm, TLA 100.2 rotor; Beckman Instruments, Palo Alto, CA) for 30 min at 20°C. Next, the pellet was quick-frozen, deep-etched, and rotary-shadowed with platinum-carbon (9–11). For the microtubules only, we used polymerized microtubules (final 2.4 mg/ml) in PEM buffer supplemented with 1 mM GTP at 37°C. Both replicas were examined by transmission electron microscopy (TEM) at a magnification of 100,000× (JEOL 2000EX). To examine for the occurrence of various types of kinesin head-decorated microtubules, photographs were taken at 40,000× without searching for any specific type. Images were recorded on Fuji FG film.

In order to observe microtubule structure in vivo, we prepared fresh and Triton-extracted samples. Slices of 4-wk-old mouse cerebellum were immersed in 1% Triton in PEM buffer, containing 10 μM taxol, for 10 min at 20°C (10). After that, for the kinesin decoration, the samples were incubated in the same buffer containing 1 mM AMP-PNP and 1.2 mg/ml of kinesin head for 5 min. Just before the freezing, samples were washed with the first buffer. Procedures are the same as the method for polymerized microtubules.

Image Filtering

Film-recorded images were digitized using a CCD camera (Eikonix 1412, Kodak) at a step size of 7 μm, corresponding to 0.7 Å. The resultant image, which contained 15–20 repeats (1,500–2,000 pixels), was included in 256 × 2,048 pixels on which two-dimensional fast Fourier transform was performed. Image analysis was carried out using software developed by Medical Research Council (Cambridge, UK); being implemented on Apollo DN5500vs and HP/Apollo 9000 series 425t workstations and a ConvexAVS image processing system operated on a C3-J computer (Convex Inc., Richardson, TX).

Fig. 3 *c* shows the amplitude map of the Fourier transform, where layer-lines with a spacing of Y = 1/4 and 1/8 nm are observed, indicating that the image can be considered to be a one-dimensional crystal structure in which the pitch along protofilaments is 8 nm. In the subsequent inverse Fourier transform, a translationally filtered image was produced by combining only the components consistent with the translational symmetry (1, 26). Generated images are shown in Fig. 3 *b*.

Results

Recombinant Mouse Kinesin Head

The expressed protein by SDS-PAGE revealed a molecular mass (40 kD) predicted from its sequence, and also displayed typical kinesin properties such as microtubule binding and microtubule-dependent activation of ATPase (data not shown). SDS-PAGE additionally showed the binding stoichiometry to be one kinesin head per tubulin dimer consistent with the previous results studied by Harrison et al. (7) (data not shown). To confirm the specific binding to β-tubulin, the kinesin head and microtubule were cross-linked with a zero-length cross-linker (Fig. 1, *a* and *b*). We found the major cross-linked product to be a new complex comprised of a single kinesin head and a tubulin monomer (90 kD). This band was specifically stained by an antibody against β-tubulin, but not by one against α-tubulin (Fig. 1 *b*).

Surface Image of Kinesin Head Decorated Microtubules

High-contrast, high-resolution TEM results of the quick-frozen, deep-etched kinesin head–decorated microtubules enabled characterization of their surface structure; thereby revealing individual macromolecules. Fig. 2 *b* shows a kine-

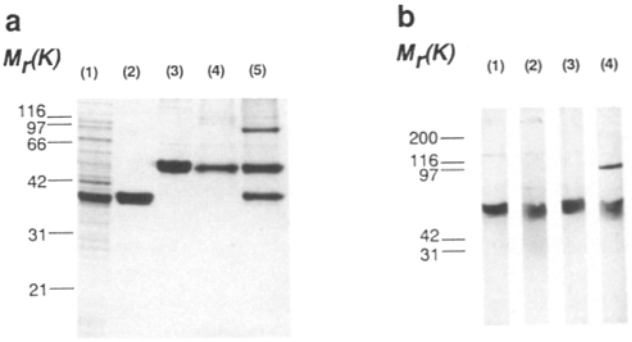

Figure 1. (*a*) Purification of the kinesin head domain (lanes *1* and *2*) and its cross-linking to microtubules (lanes *3–5*). (Lane *1*) Crude supernatant of *E. coli*-expressed kinesin head. (Lane *2*) His-tag–purified kinesin head (40 kD). (Lane *3*) Microtubule (50 kD). (Lane *4*) Cross-linked microtubule (50 kD). (Lane *5*) Cross-linked microtubule and kinesin head. In addition to tubulin (50 kD) and the kinesin head (40 kD), a new 90-kD band was recognized. (*b*) Immunoblots showing crosslinking of the kinesin head to β-tubulin using 1-ethyl-3-[3-(dimethylamino)propyl]carbodiimide. (Lane *1*) Cross-linked microtubule alone stained by DM1A (anti-α-tubulin). (Lane *2*) Cross-linked microtubule stained by DM1B (anti-β-tubulin), (Lane *3*) Cross-linked microtubule and the kinesin head stained by DM1A. (Lane *4*) Cross-linked microtubule and the kinesin head stained by DM1B. Note that only the anti-β-tubulin antibody stained cross-linked tubulin and the kinesin head (90 kD).

1. *Abbreviations used in this paper*: a.a., amino acids; AMP-PNP, 5′-adenylyl-β,γ-imidodiphosphate; MAP, microtubule-associated protein; TEM, transmission electron microscopy.

sin head-decorated microtubule with no apparent discontinuities. In comparison to a microtubule without a decoration (Fig. 2 *a*), note the clearly distinguished 5–6-nm-diam particles. These particles are believed to be kinesin heads that are so uniformly aligned along the microtubule longitudinal axis at a 8-nm pitch that no breaks can be seen. It should be realized that this pitch corresponds to that of β-tubulin along a microtubule protofilament. However, in the microtubule of the B lattice model (based on the lateral interaction of homo subunits), the helix of kinesin heads is at a shallow angle (~9°), and therefore this helix should have a 12-nm pitch. Since the pitch of the helix and protofilament are obviously different and not multiples of each other, there should be at least one helical discontinuity per turn. We found that such a discontinuity emerges as a "seam line," i.e., a line formed when kinesin heads on the adjoining protofilaments are in a staggered arrangement (indicated with an *arrowhead* in Fig. 2 *c* and with *arrows* in Fig. 3 *a*, lanes *3–6*). To better confirm this interesting feature, we translationally filtered these images along their longitudinal axis (Fig. 3 *b*), with the seam line becoming much more prominent (Fig. 3 *b*, lanes *3–6*). The heads are staggered at about a half-pitch aberration (4 nm). Surprisingly, some microtubules showed a "double seam line" (Fig. 3 *a*, lanes *7–9*), where the heads are staggered on both sides of a protofilament, being a distinct feature in the filtered images (Fig. 3 *b*, lanes *7–9*). Because the number of seam lines should be odd, a third seam line should exist on the other side of the microtubule (see Discussion). Consequently, a microtubule with double seam line has at least two, and is postulated to have three seam lines.

To examine the lattice structure of microtubules in vivo, kinesin head decoration was applied to the microtubules in mouse cerebella. Fig. 4 shows microtubules in nerve cell processes. Surprisingly even in the presence of other microtubule-associated proteins (MAPs) which are seen as crossbridges between the microtubules (Fig. 4, *a–c*), kinesin head fully decorated the microtubules (Fig. 4 *b*). The lattice structure is the same as in vitro. As expected, seam lines are also found in vivo (Fig. 4 *c*).

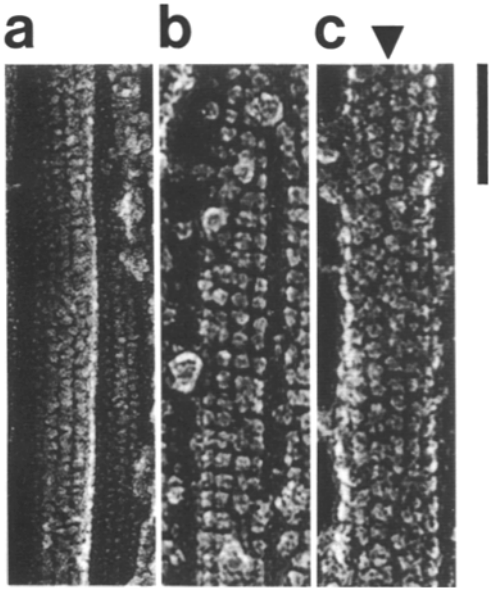

Figure 2. Electron micrographs of quick-freeze, deep-etch replicas of (*a*) a microtubule, (*b*) a kinesin head-decorated microtubule showing a continuous helical lattice (B lattice), and (*c*) kinesin head-decorated microtubule with the helical discontinuity appearing as a seam line (indicated by *arrowhead*). Bar, 50 nm.

Occurrence of Seam Lines

Among the 13 or 14 protofilaments in a microtubule, only three or four protofilaments could be seen from one side (Fig. 5 *b*), i.e., assuming that there is one seam line per microtubule, the frequency of observing it should be <3/14 (21%). Among the 235 microtubules we observed in vitro, 36 microtubules had a seam line (16%), whereas only three had a double seam line (1.3%). Interestingly, no nonadjacent seam lines were found. These results strongly suggest that all microtubules have at least one seam line, and infrequently more than one.

Discussion

Microtubule Lattice

As a result of our unique findings, we classify inter-protofilament bonds on " A lattice bond" or "B lattice bond," which respectively correspond to the lateral bond between heterologous tubulins (α-β) or homologous tubulins (α-α and β-β) in A or B lattice microtubules. A seam line in a B lattice microtubule, where neighboring tubulin dimers are in a staggered arrangement, is therefore considered to be an A lattice bond. Use of these terminologies enables the lattice property of microtubules to be quantitatively represented as the number of respective bonds.

In the previous study, Song and Mandelkow (23) carried out negative staining of the kinesin head–microtubule complex, and the result indicated that a reassembled microtubule has a B lattice structure. They based their conclusion on the near-meridional spot observed on an 8-nm layer line located midway between the origin and the J_3 reflection occurring on a 4-nm layer line; a finding that indicates the B lattice bonds are dominant in a microtubule. A question remains, though, as to how many A lattice bonds exist in a microtubule, since the presence of this near-meridional spot cannot rule out the existence of a mixed lattice microtubule having more than one A lattice bond (18). In fact, we found the existence of a microtubule with a double seam line, i.e., having at least two (assumed to have three) A lattice bonds in vitro.

In contrast, use of quick-freeze, deep-etch EM is comparatively more advantageous to examine this type of asymmetric structure, because it can resolve individual macromolecules. In addition, it can selectively visualize the upper side of the microtubule, which makes image analysis easier. Thus, even if discontinuities were randomly distributed over the microtubule wall, they could have been visualized. Use of this method also enables us to visualize the lattice structure in vivo such as in nerve cells in mouse cerebella which would be impossible by other methods.

As in the previous studies, the *E. coli* expressed NH_2-terminal fragment of kinesin heavy chain was also used for β-tubulin marker, but its property should be considerably different from others. Here the 340-a.a. residues of mouse kinesin was used, while the 401-a.a. residues of *Drosophila*

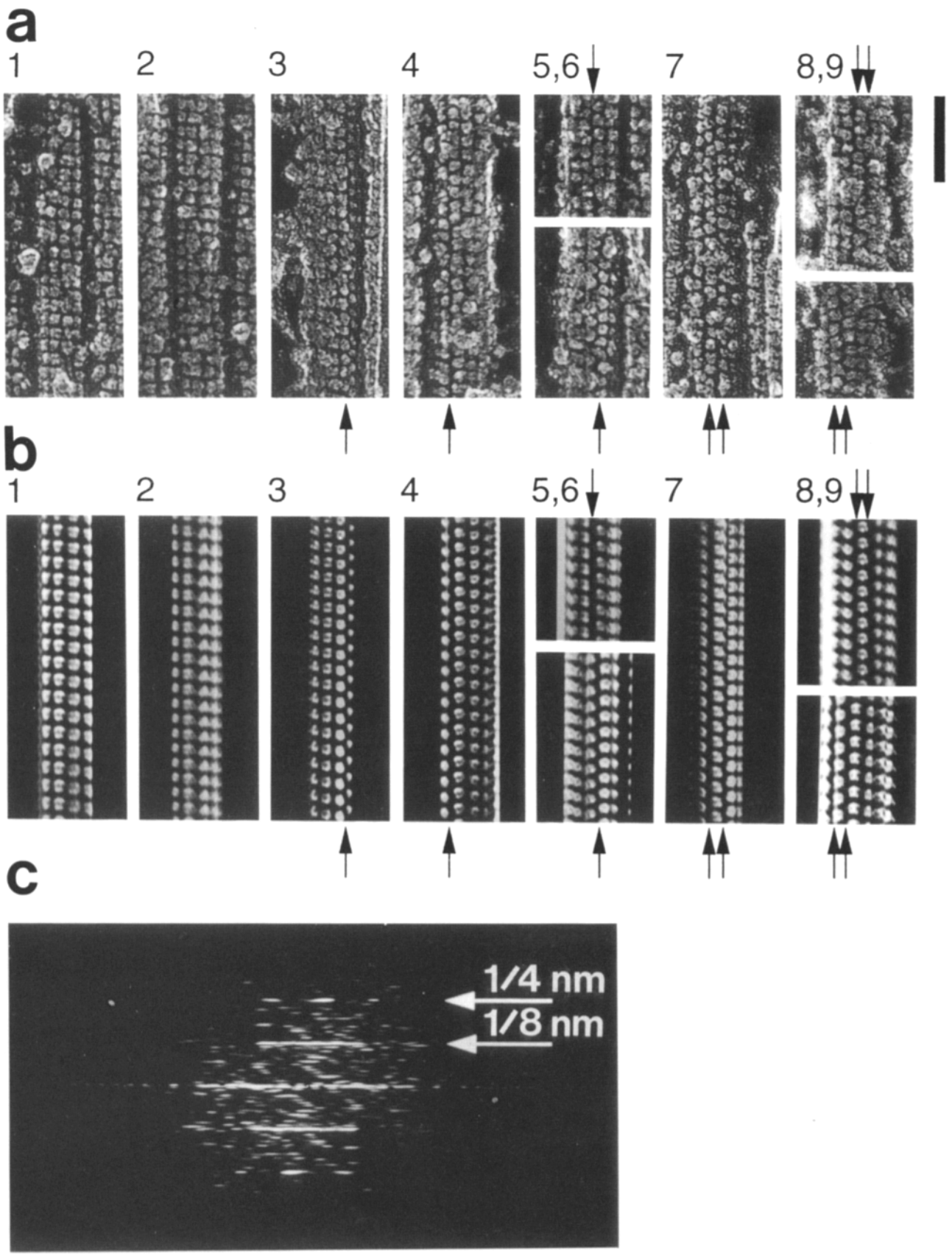

Figure 3. (*a*) Electron micrographs of freeze-fracture replicas of kinesin head-decorated microtubules. Seam lines are indicated by arrows at 3–9, but not at 1 and 2, presumably because they are situated on the other side. (*b*) Translationally filtered images of *a*. Only the Fourier components consisted with the translational symmetry, i.e., the layer-lines with a spacing of 1/4 and 1/8 nm and the equator, were combined

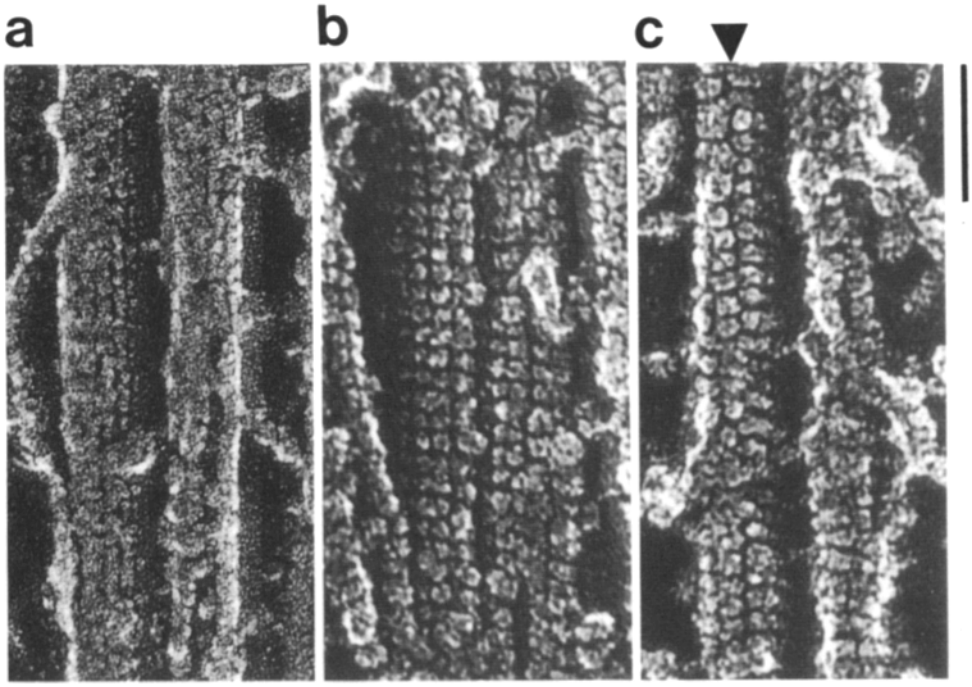

Figure 4. (*a*) Nondecorated microtubules; (*b*) kinesin head–decorated microtubules showing a continuous helical lattice (B lattice); and (*c*) a kinesin head–decorated microtubule with a seam line (indicated by *arrowhead*) in nerve cells in mouse cerebella. Bar, 50 nm.

kinesin (7) and the 395-a.a. residues of squid kinesin (23) were used in the previous studies. Huang et al. showed that the 340-a.a. residues protein of *Drosophila* kinesin is monomeric, while the 392-a.a. residues protein is dimeric (13). Therefore, the fragment used here thought to be monomeric while dimeric one was used in the previous two studies, since the amino acid sequences of the kinesin head domain are highly conserved among these species (67% identity and 81% similarity). The monomer kinesin head may make our chemical cross-linking so specific that a band composed of one β-tubulin and one kinesin head was clearly distinguished both in SDS-PAGE and in Western blotting. The smallness of the kinesin head should have also contributed to avoid the steric hindrance on a microtubule. Actually it is difficult to observe clear 8-nm longitudinal pitch on the microtubules decorated with longer fragment (450 a.a) of kinesin by quick-freeze, deep-etch EM (data not shown).

As a whole, our results clearly indicate that a microtubule structure is a complex of A and B lattice bonds. Most microtubules, having 13 or 14 protofilaments, should have at least one A lattice bond appearing as a seam line and 12 or 13 B lattice bonds both in vitro and in vivo. These data suggest that the lateral bonds have enough flexibility to allow both A and B lattice bonds.

Possible Roles of Seam Lines

What are the roles of seam lines? One possibility is that it defines the potential attachment site of some MAPs. There are several lines of evidence that microtubules in vivo are asymmetric; flagellar A-tubule has specific nontubulin proteins that are associated with the resistant three-protofilament ribbons (15). The central-pair apparatus of squid sperm flagella has microtubule-associated "sheath" components along a protofilament (16). These asymmetric components may attach to seam lines and/or they induce the formation of seam lines. As for the microtubules in nerve cells, it seems that such components do not exist as major constituent, since no structure has been observed that is aligned parallel to the protofilaments and the kinesin head decoration was not interfered with MAPs at the seam line. But there is still a possibility of existence of minor components. Such components may attach the seam lines to stabilize the microtubules and may control the polymerization–depolymerization cycles within neuronal processes during growing phase or in cells during mitosis.

Double Seam Lines

The appearance of the double seam line is of particular interest, since this structure can not be predicted from the simple B lattice model. Fig. 5 *a* shows a model of the double seam line, where it should be noted that the underlying tubulin monomers have a three-start helix structure, being the same structure as that generally observed in a monomer lattice. Also, note that three protofilaments are bound with two A lattice bonds, two of them are on the upper side, and another is on the lower side. Should this model hold, the double seam line could have a local A lattice structure comprised of three protofilaments. As indicated, the helix of the monomer is a three-start helix, and consequently, the number of A lattice bonds should be odd; and probably the third A lat-

to produce the filtered image. The height of the rectangular mask along the meridian was 1/70 $Å^{-1}$. Seam lines be clearly appear at 3–9. (*c*) Computed diffraction pattern synthesized from the image shown in *a* at 3. Layer lines are clearly observed with a spacing of 1/4 and 1/8 nm along the meridian, which indicates that the image can be interpreted to be a one-dimensional crystal. Bar, 50 nm.

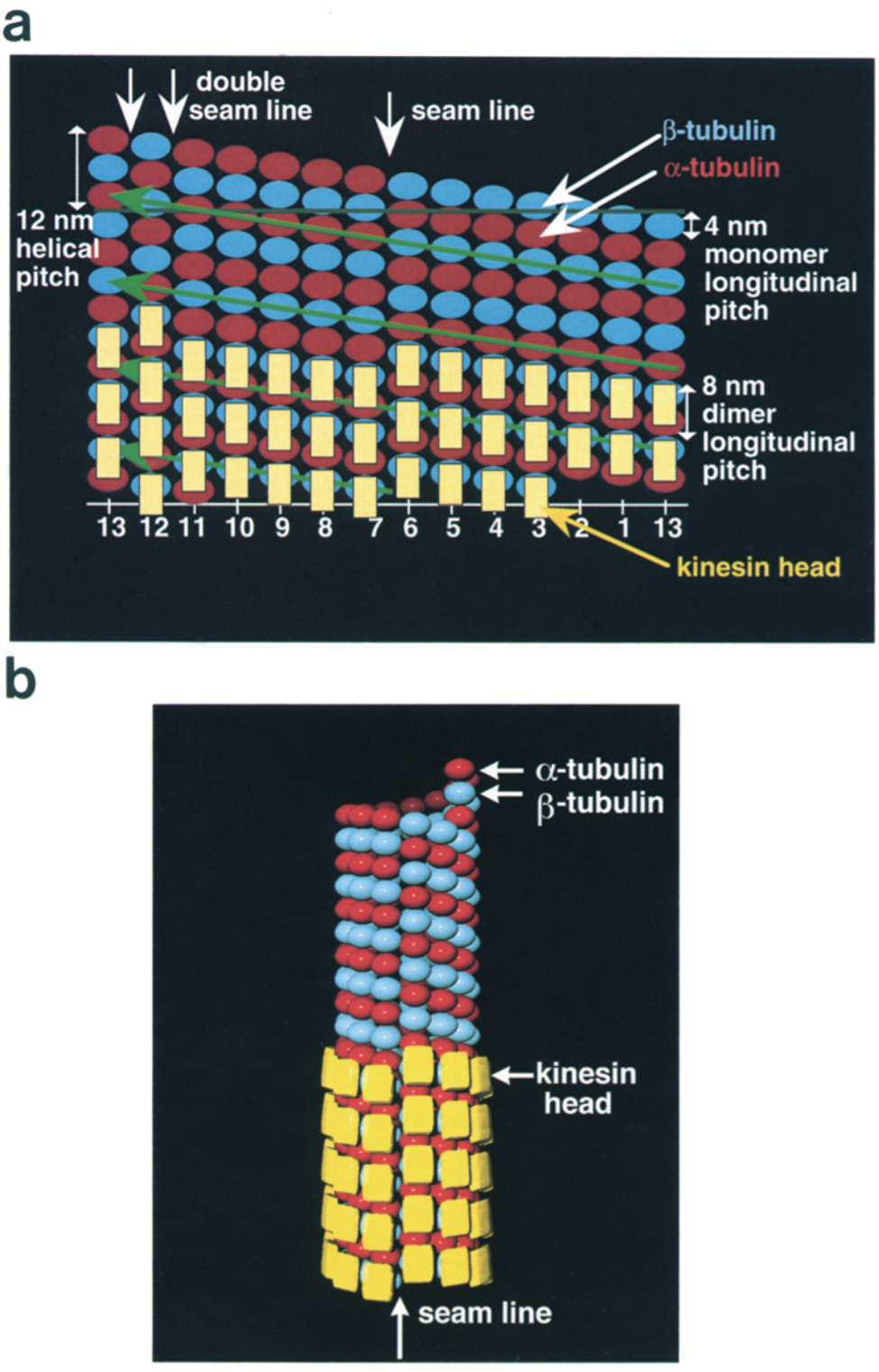

Figure 5. (*a*) The extended lattice model of a microtubule (upper part), and the model of a kinesin head-decorated microtubule (lower part). Angled green arrows indicate a continuous helix. (*b*) Tube lattice labeled the same as in *a*.

tice bond is situated on the other side of the microtubule. As for the in vivo microtubule, we did not observe the double seam line in vivo, but due to the relatively small number of microtubules clearly decorated with kinesin head compared with those in vitro, we can not exclude the existence of double seam lines. Even if it does not exist in vivo, still we think the structure reflects the tubulin property in the absence of MAPs.

Tubulin–Motor Protein Interactions

Microtubule surface lattice also plays important roles as a track for motor proteins such as kinesin and dynein. Kinesin follows the microtubule's protofilament axis from minus- to plus-end (19), while dynein moves with 1.85 ± 0.45 rotation for every micrometer of axial movement plus- to minus-end (25). Thus, how these motor proteins interact with

microtubules is essential to understand the mechanism of mechanochemical coupling.

Then does kinesin head interact with the ridge on one protofilament or with the groove among two protofilaments? In another words, does it use one protofilament or two protofilaments as a track? Our results provide two keys for answering the question: (*a*) the kinesin head binds tightly to one β-tubulin according to the chemical cross-linkage; and (*b*) the kinesin head binds to protofilaments even at the seam line(s) (this is why we could clearly visualize the seam line). From *a*, we can conclude that the β-tubulin in one protofilament serves as a main binding site for a kinesin head. Then, from *b*, either an α- or β-tubulin constitute the protofilament adjacent to the β-tubulin, that a kinesin head binds to, i.e., β-tubulin does so at the B lattice bond and α-tubulin at the A lattice bond (see Fig. 4 *a*, in which the right side of the kinesin head is usually β-tubulin, while being α-tubulin at the seam line). Our results show that a kinesin head binds to one β-tubulin no matter which tubulin is adjacent to it. Therefore, it is likely that a kinesin uses only one protofilament as a track. The exact answer can be elucidated by the three dimensional reconstruction of the kinesin head and microtubule complex.

The rotational movement of dynein, which is not parallel to the protofilament, postulates an important question on lattice–motor interaction when we consider the existence of seam lines. The averaged rotation rate implies that dynein changes the track to the neighboring protofilament for every five tubulin dimer units of axial movement (25). In addition, dynein should go across a seam line for every 70 tubulin dimer units of axial movement approximately, even though the microtubule surface lattice is discontinuous there. It may be because dynein interacts more weakly with microtubules than kinesin does as was shown by assaying microtubule movement when intermediate states in the hydrolysis cycle are prolonged with ATP analogues or inhibitors (20). Still further study is required to clarify the relationship between seam lines and dynein movement.

Although the exact function of seam lines are speculative, the existence itself gives us the keys to answer the fundamental questions regarding the interaction between microtubules and microtubule binding proteins such as MAPs and motor proteins.

Sincere gratitude is extended to Dr. K. Kato for providing cDNA of mouse kinesin. We thank S. Nonaka for drawing figures.

M. Kikkawa was supported by a fellowship of the Japan Society for the Promotion of Science for Japanese Junior Scientists and by the Recruit Scholarship Foundation. T. Ishikawa was also on a JSPS fellowship. This work was supported by the grants-in-aid for specially promoted projects from the Ministry of Education, Science and Culture of Japan to N. Hirokawa and to T. Wakabayashi, and grants from RIKEN to N. Hirokawa and T. Wakabayashi (Biodesign).

Received for publication 27 May 1994 and in revised form 30 September 1994.

References

1. Amos, L., and A. Klug. 1972. Image filtering by computer. *Proc. Fifth Eur. Congr. Electron Microscopy*. 580–581.
2. Amos, L., and A. Klug. 1974. Arrangement of subunits in flagellar microtubules. *J. Cell Sci.* 14:523–549.
3. Amos, L. 1979. Structure of microtubules. *In* Microtubules. K. Roberts and J. Hyams, editors. Academic Press. London. 1–66.
4. Beese, L., G. Stubbs, and C. Cohen. 1987. Microtubule structure at 18 Å resolution (and see erratum, 1988. *J. Mol. Biol.* 199:547). *J. Mol. Biol.* 194:257–264.
5. Chrétien, D., and R. Wade. 1991. New data on the microtubule surface lattice (and see erratum, 1991. *Biol. Cell.* 72:284). *Biol. Cell.* 71:161–174.
6. Erickson, H. P. 1974. Microtubule surface lattice and subunit structure and observations on reassembly. *J. Cell Biol.* 60:153–167.
7. Harrison, B., S. Marchese-Ragona, S. Gilbert, N. Cheng, A. Steven, and K. Johnson. 1993. Decoration of the microtubule surface by one kinesin head per tubulin heterodimer. *Nature (Lond.)*. 362:73–75.
8. Herzog, W., and K. Weber. 1978. Fractionation of brain microtubule-associated proteins. Isolation of two different proteins which stimulate tubulin polymerization in vitro. *Eur. J. Biochem.* 92:1–8.
9. Heuser, J., and S. Salpeter. 1979. Organization of acetylcholine receptors in quick-frozen, deep-etched, and rotary-replicated Torpedo postsynaptic membrane. *J. Cell Biol.* 82:150–173.
10. Hirokawa, N. 1982. Cross-linker system between neurofilaments, microtubules, and membranous organelles in frog axons revealed by the quick-freeze, deep-etching method. *J. Cell Biol.* 94:129–142.
11. Hirokawa, N., Y. Shiomura, and S. Okabe. 1988. Tau proteins: the molecular structure and mode of binding on microtubules. *J. Cell Biol.* 107:1449–1459.
12. Hirokawa, N., K. Pfister, H. Yorifuji, M. Wagner, S. Brady, and G. Bloom. 1989. Submolecular domains of bovine brain kinesin identified by electron microscopy and monoclonal antibody decoration. *Cell.* 56:867–878.
13. Huang, T. G., J. Suhan, and D. D. Hackney. 1994. Drosophila kinesin motor domain extending to amino acid position 392 is dimeric when expressed in Escherichia coli. *J. Biol. Chem.* 269:16502–16507.
14. Kato, K. 1991. Sequence analysis of twenty mouse brain cDNA clones selected by specific expression patterns. *Eur. J. Neurosci.* 2:704–711.
15. Linck, R. W. 1976. Flagellar doublet microtubules: fractionation of minor components and alpha-tubulin from specific regions of the A-tubule. *J. Cell Sci.* 20:405–439.
16. Linck, R. W., G. E. Olson, and G. L. Langevin. 1981. Arrangement of tubulin subunits and microtubule-associated proteins in the central-pair microtubule apparatus of squid (Loligo pealei) sperm flagella. *J. Cell Biol.* 89:309–322.
17. Mandelkow, E., R. Schultheiss, R. Rapp, M. Muller, and E. Mandelkow. 1986. On the surface lattice of microtubules: helix starts, protofilament number, seam, and handedness. *J. Cell Biol.* 102:1067–1073.
18. McEwen, B., and S. Edelstein. 1980. Evidence for a mixed lattice in microtubules reassembled in vitro. *J. Mol. Biol.* 139:123–145.
19. Ray, S., E. Mayhofer, R. Milligan, and J. Howard. 1993. Kinesin follows the microtubule's protofilament axis. *J. Cell Biol.* 121:1083–1093.
20. Romberg, L., and R. D. Vale. 1993. Chemomechanical cycle of kinesin differs from that of myosin. *Nature (Lond.)*. 361:168–170.
21. Scholey, J., J. Heuser, J. Yang, and L. Goldstein. 1989. Identification of globular mechanochemical heads of kinesin. *Nature (Lond.)*. 338:355–357.
22. Shelanski, M., F. Gaskin, and C. Cantor. 1973. Microtubule assembly in the absence of added nucleotides. *Proc. Natl. Acad. Sci. USA*. 70:765–768.
23. Song, Y., and E. Mandelkow. 1993. Recombinant kinesin motor domain binds to beta-tubulin and decorates microtubules with a B surface lattice. *Proc. Natl. Acad. Sci. USA*. 90:1671–1675.
24. Vale, R., T. Reese, and M. Sheetz. 1985. Identification of a novel force-generating protein, kinesin, involved in microtubule-based motility. *Cell.* 42:39–50.
25. Vale, R. D., and Y. Y. Toyoshima. 1988. Rotation and translocation of microtubules in vitro induced by dyneins from Tetrahymena cilia. *Cell.* 52:459–469.
26. Wakabayashi, T., M. Kubota, M. Yoshida, and Y. Kagawa. 1977. Structure of ATPase (coupling factor TF1) from a thermophilic bacterium. *J. Mol. Biol.* 117:515–519.
27. Yang, J. T., W. M. Saxton, R. J. Stewart, E. C. Raff, and L. S. Goldstein. 1990. Evidence that the head of kinesin is sufficient for force generation and motility in vitro. *Science (Wash. DC)*. 249:42–47.